



Sharif University of Technology
Scientia Iranica
Transactions B: Mechanical Engineering
<http://scientiairanica.sharif.edu>



Investigation of particle deposition and dispersion using hybrid LES/RANS model based on lattice Boltzmann method

H. Sajjadi^{a,*}, M. Salmanzadeh^b, G. Ahmadi^c, and S. Jafari^d

a. *Department of Mechanical Engineering, Faculty of Engineering, University of Bojnord, Bojnord, P.O. Box 94531-55111, Iran.*

b. *Department of Mechanical Engineering, Shahid Bahonar University of Kerman, Kerman, Iran.*

c. *Department of Mechanical and Aeronautical Engineering, Clarkson University, Potsdam, NY, USA.*

d. *Department of Petroleum Engineering, Shahid Bahonar University of Kerman, Kerman, Iran.*

Received 17 February 2018; received in revised form 10 March 2018; accepted 21 July 2018

KEYWORDS

Hybrid RANS/LES;
LBM;
Particle deposition;
Particle dispersion.

Abstract. In this study, a new hybrid RANS/LES turbulence model within the framework of the Multi Relaxation Time (MRT) Lattice Boltzmann Method (LBM) was used to study particle dispersion and deposition in a room. For the hybrid RANS/LES method, the near-wall region was simulated by the RANS model, while the rest of the domain was analyzed using the LES model within the framework of the LBM. In the near-wall layer where RANS was used, the $k - \varepsilon$ turbulence model was employed. To simulate the particle dispersion and deposition in the room, particles with diameters of 10 nm to 10 μm were investigated. The simulated results for particle dispersion and deposition showed that the predictions of the present hybrid method were quite similar to those of earlier LES-LBM. In addition, the predictions of the hybrid model for the particle deposition and dispersion were closer to LES simulation results, as compared to those of the $k - \varepsilon$ model.

© 2018 Sharif University of Technology. All rights reserved.

1. Introduction

It is well known that people spend more than 85% of their time indoors, and most of their exposure to environmental pollutants occurs by breathing the indoor air. Therefore, Indoor Air Quality (IAQ) has received increasing attention in recent years as an important public health issue. In the last decade, Computational Fluid Dynamics (CFD) has become a powerful tool for studying IAQ under various conditions [1-4].

The Lattice Boltzmann Method (LBM) is a relatively new, efficient, and convenient computational model that has increasingly attracted the attention of researchers in different areas. The LBM has been used to simulate turbulent flows, multi-phase flows, single and multiphase flows in porous media, and particulate suspensions in the past two decades [5,6]. The most widely used method for simulating indoor airflows is to solve the Reynolds-Averaged Navier-Stokes (RANS) equation in conjunction with the use of a turbulence model. Among various RANS turbulence models, the two-equation $k - \varepsilon$ model is the most popular one. The RANS model, however, simulates the mean flow velocity and mean-square fluctuation fields; however, it cannot predict the fluctuating velocity field [7].

For using the $k - \varepsilon$ model in the framework of LBM, two approaches have been used. In most earlier

*. *Corresponding author. Fax: +98 5832410700*
E-mail addresses: H.sajjadi@ub.ac.ir (H. Sajjadi);
msalmanz@clarkson.edu (M. Salmanzadeh);
Gahmadi@clarkson.edu (G. Ahmadi);
saeed.jafari.1362@gmail.com (S. Jafari)

works, a separate finite difference grid is created to solve the $k - \varepsilon$ (or other) transport equations and, then, return the calculated values into the LBM framework for evaluating the eddy viscosity and turbulent stresses [8,9]. Recently, a new method has been suggested in [10-12] that introduces two additional populations for k and ε and solves the $k - \varepsilon$ equations within the LBM with no need for a new grid.

The Large Eddy Simulation (LES) is run for the large eddies, and it only models the fluctuations that are smaller than the grid size. The LES approach typically provides more accurate results for airflow modeling than the RANS models do, and it also provides the turbulent fluctuation velocity that is larger than the grid size. Due to these advantages, the use of LES model for simulating indoor airflows has markedly increased in the last decade [13-15]. The LES model in framework of LBM was also used to investigate turbulent flows for different applications [16,17]. The major difficulty with using LES for simulating the indoor airflow is that resolving the problem of near-wall flows requires a very fine grid to capture large eddies, which increase the computation cost significantly [18].

As noted earlier, while the LES model leads to accurate results, the required computation times are quite high. The RANS model, however, does not provide information on the instantaneous fluctuation velocity field. To overcome the disadvantages of LES and RANS, the hybrid RANS/LES concept was introduced to simulate flow in the past decade [19,20]. The basic idea of the hybrid model is to use the LES model in the bulk of the domain, while the RANS model is used to simulate the near-wall regions to avoid the need for a very high-resolution grid. For the RANS region, different models, such as $k - \varepsilon$, $k - \omega$, Spalart-Allmaras (SA), and $v2f$ models, were used [21,22]. Recently, Sajjadi et al. [18] developed the hybrid RANS/LES model within the LBM framework to solve the problem of turbulent flows in the indoor environment, where the $k - \varepsilon$ -LBM and LES-LBM models were used. They concluded that the computation cost of using the hybrid model is considerably lower than that of the LES; however, it is higher than that of the RANS approach. In this respect, the accuracy of the hybrid RANS/LES predictions is much higher than that of RANS, yet somewhat lower than that of LES. In addition, they showed that the new hybrid model predicted the large-scale fluctuation velocity field cost effectively when compared with the LES.

Particle dispersion and deposition in turbulent flows and, in particular, in the indoor environment has attracted considerable attention in recent years [23-26]. Fan and Ahmadi [27] proposed a sub-layer model to capture the effect of near-wall vortical structure of turbulent flows on particle deposition in vertical ducts. Zhang and Ahmadi [28] used the direct numerical

simulation technique for simulating particle deposition in turbulent duct flows. Salmanzadeh et al. [29] showed the effect of subgrid scale (SGS) model on the Large Eddy Simulation (LES) of particle deposition in turbulent channel flow. Recently, Sajjadi et al. [12] developed a new $k - \varepsilon$ -LBM method and simulated particle deposition in turbulent channel flows and found reasonable agreement with the earlier numerical and experimental results. In addition, Sajjadi et al. [11] investigated particle transport in a modeled room using the LES-LBM and the $k - \varepsilon$ -LBM approaches. They showed that both methods predicted particle dispersion and deposition in the indoor environment reasonably well.

Applications of hybrid RANS-LES within the LBM for particle dispersion and deposition have not been tested yet. The main aim of this work is to use the hybrid RANS-LES within the LBM framework to investigate the particle transport processes in an indoor environment. The Lagrangian particle tracking approach was also used in these simulations, and the dispersion and deposition of particles of different sizes were studied. For nanoparticles, the effect of the Brownian excitations was included in the analysis. It was shown that the hybrid-LES- $k - \varepsilon$ -LBM model predicted the particle deposition more accurately than the $k - \varepsilon$ -LBM did; however, while being computationally more economical, it predicted the particle deposition slightly less accurately than the LES-LBM did.

2. Hybrid LES/RANS model based on LBM

To reduce the computation cost of simulations while maintaining the accuracy, the hybrid LES/RANS model is used. In other words, the LES with a subgrid-scale model is used for bulk of the flow region, while the RANS model is used for the near-wall regions. In this study, the LBM- $k - \varepsilon$ model was used to analyze the RANS near-wall region, and the MRT-LBM-LES model was used for simulating the bulk of the flow region. Sajjadi et al. [11,12,18] described details of the LBM- $k - \varepsilon$, MRT-LBM-LES, and the hybrid models of flow simulations. Therefore, only a brief summary is outlined.

For the LBM- $k - \varepsilon$ model, two additional distribution functions for the k and ε are defined as follows:

$$k = \sum_i g_i, \quad (1)$$

$$\varepsilon = \sum_i h_i. \quad (2)$$

The transport equations for the new distribution functions are:

$$g_i \left(x + c_i \Delta t, t + \Delta t \right) - g_i(x, t)$$

$$= -\frac{1}{\tau_k} [g_i(x, t) - g_i^{eq}(x, t)] + \Delta t F_i, \quad (3)$$

$$h_i\left(x + c_i \Delta t, t + \Delta t\right) - h_i(x, t) = -\frac{1}{\tau_\varepsilon} [h_i(x, t) - h_i^{eq}(x, t)] + \Delta t F_i, \quad (4)$$

For k :

$$F_i = \omega_i (\nu_t |S|^2 - \varepsilon) \left(1 + \frac{c_i \cdot u}{C_s^2} (\tau_k - 0.5) / \tau_k\right), \quad (5)$$

For ε :

$$F_i = \omega_i \left(C_1 \frac{\varepsilon}{k} (\nu_t |S|^2) - C_2 \frac{\varepsilon^2}{k}\right) \left(1 + \frac{c_i \cdot u}{C_s^2} (\tau_\varepsilon - 0.5) / \tau_\varepsilon\right). \quad (6)$$

Herein, $C_1 = 1.44$, $C_2 = 1.92$, and the turbulence kinematic viscosity for RANS model is given as follows:

$$\nu_t = C_\mu \frac{k^2}{\varepsilon}.$$

For the MRT-LBM-LES, to evaluate the distribution function, the following transport equation is used:

$$f_i(x + c_i \Delta t, t + \Delta t) = f_i(x, t) - M_{ij}^{-1} \cdot \hat{S}_{jk} \cdot [R_k(x, t) - R_k^{eq}(x, t)]. \quad (7)$$

Components of R_k , R_k^{eq} , M_{ij} , \hat{S}_{jk} , subgrid scale viscosity $\nu_i^{SG} = (C_s \Delta)^2 |S|$, and strain rate norm $|S|$ are described in [11,18], where $C_s = 0.16$ and $\Delta = (\Delta x \Delta y \Delta z)^{1/3}$.

In the new hybrid method, the transport equations for k and ε are solved in the entire flow domain, and the distribution function for the MRT-LBM-LES is solved in bulk of the flow region. In addition, very close to the walls, the standard wall function was used [12].

To switch between the MRT-LBM-LES and the LBM- $k - \varepsilon$ models, a linear interpolation based on the y^+ value is used [30]. In other words,

$$\nu_t = \begin{cases} \nu_{t,LES} & \text{if } y^+ > y_{up}^+ \\ (1-\beta)\nu_{t,k-\varepsilon} + \beta\nu_{t,LES} & \text{if } y_{down}^+ < y^+ < y_{up}^+ \\ \nu_{t,k-\varepsilon} & \text{if } y^+ < y_{down}^+ \end{cases} \quad (8)$$

where β is the weighting factor:

$$\beta = \frac{y^+ - y_{down}^+}{y_{up}^+ - y_{down}^+}. \quad (9)$$

Herein, y_{down}^+ and y_{up}^+ are respectively the lower and upper limits of transition region in wall units selected as 60 and 300 [30].

3. Particle motions

The equation of motion of small particles is given by [11]:

$$\frac{du_{pi}}{dt} = \frac{1}{\tau_p} \frac{C_D Re_p}{24} (u_{fi} - u_{pi}) + \left(1 - \frac{1}{S}\right) g_i + n_i(t), \quad (10)$$

where u_{pi} is the particle velocity, u_{fi} is the instantaneous airflow velocity in the particle location, τ_p is the particle relaxation time, given as: $\tau_p = \frac{S d^2 C_c}{18 \nu}$, and S is the ratio of particle density to fluid density. Herein, C_c is the Cunningham slip correction and is given as follows:

$$C_c = 1 + \frac{2\lambda}{d} (1.257 + 0.4e^{-\frac{1.1d}{\lambda}}).$$

In Eq. (10), C_D is the drag coefficient and defined as follows:

$$C_D = \frac{24}{Re_p} \quad Re_p < 1, \quad (11)$$

$$C_D = \frac{24}{Re_p} (1 + 0.15 Re_p^{0.687}) \quad 1 < Re_p < 400, \quad (12)$$

where Re_p is the particle Reynolds number that is defined as:

$$Re_p = \frac{d |u_{rel}|}{\nu} \quad u_{rel} = u_j - u_j^p.$$

In Eq. (10), the drag force, the buoyancy force, and the Brownian force are included in the particle equation of motion; however, the lift force, which is comparatively small, is neglected [11].

The first term on the right-hand side of Eq. (10) is the drag force caused by the relative motion between particles and flow. The second term on the right-hand side of Eq. (10) represents the gravitational force corrected by the buoyancy force. The third term represents the Brownian force. The Brownian excitation is very important for nanoparticles and is modeled as a Gaussian white noise random process [24]. In other words,

$$n_i(t) = \zeta_i \sqrt{\frac{\pi S_0}{\Delta t}}, \quad (13)$$

where $S_0 = \frac{216 \nu k_i T}{\pi^2 \rho d^5 (S)^2 C_c}$, and ζ is selected at every time step from a population of zero-mean, unit-variance independent Gaussian random numbers.

4. Modeled geometry

In this study, to test the newly developed method for predicting particle dispersion and deposition, a scale room model was used. This configuration is identical to that studied in [31] for examining the effectiveness of the hybrid approach for airflow simulation. As shown in Figure 1, the scaled room is roughly one-tenth scale of a full-size office with dimensions of

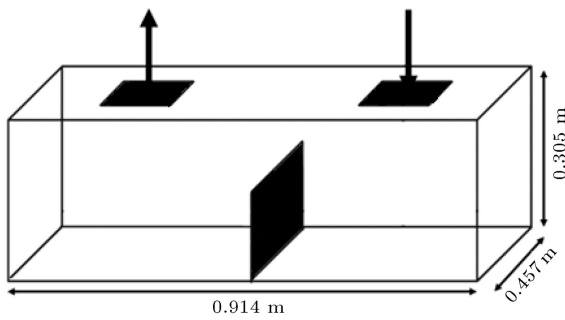


Figure 1. Geometry of the scaled room model used in the present study [31].

0.914 m \times 0.305 m \times 0.457 m. A partition with half the room height is located in the middle of the room. Ventilation air enters the room vertically from one side of the ceiling and exits through the outlet register located on the other side of the ceiling. The dimensions of the inlet and outlet are 0.101 m \times 0.101 m, and the inlet airflow velocity is typically 0.24 m/s. The corresponding Reynolds number based on the inlet length and an inlet airflow velocity is 1628.

5. Results and discussion

5.1. Flow field

Results of the airflow field in the modeled room, which is used in the present work utilizing the hybrid method, were investigated by the authors in [18]. It was shown that the hybrid LES/RANS model within the LBM framework predicted the mean flow field and the fluctuation in RMS velocities reasonably well.

5.2. Particle dispersion and deposition

In this section, particle dispersion and deposition processes for various particles sizes (10 nm, 100 nm, 1 μ m, and 10 μ m) in the room were simulated. The unsteady airflow was first simulated for about 70 s to reach a roughly quasi-steady condition; then, the particle injection was initiated with 144 particles injected uniformly at the inlet with the same velocity as the airflow at every 0.05 s. Particle injection stopped when the simulation time reached 100 s. Therefore, a total of 86,400 particles were injected into the flow.

Figure 2 compares the number of suspended 1 μ m particles in the room as predicted by different models. The earlier simulations of Sajjadi et al. [11] and Tian et al. [31] are shown in this figure for comparison. Two Boundary Conditions (BC) were used for particle-wall interactions; the first boundary condition is “reflect,” for which when a particle collides with a wall, it bounces back. This is the assumption used by Tian et al. [31]. The second BC is “trap.” When the distance of particle center from the wall reaches $d_p/2$, it is assumed that the particle is deposited on the wall. It should be pointed out that, for 1 and 10 μ m particles, the

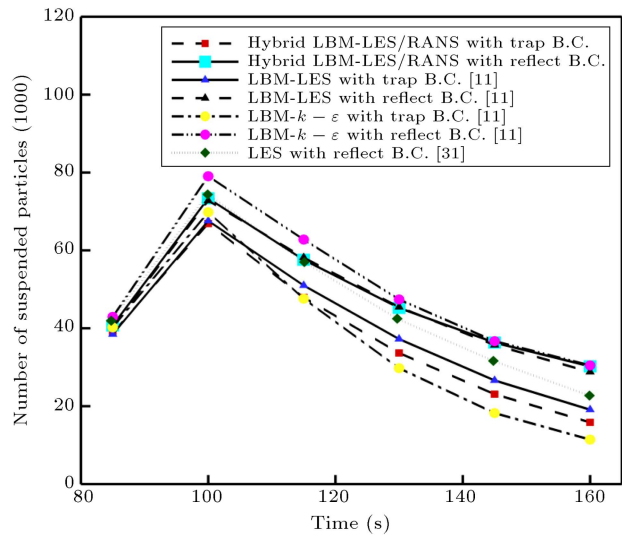


Figure 2. Comparison of the number of suspended 1 μ m particles in the room under trap and reflect boundary conditions (Total number of injected particles is 86,400 and Re_{Inlet} is 1628).

trap boundary condition is more realistic, as the van der Waals forces cause these small particles to adhere to the surface, with a little chance for rebound [27]. The reflect boundary condition here was just used to compare the present simulation results with the earlier results of Tian et al. [31].

Figure 2 clearly shows that the number of suspended particles increases with time up to $t = 100$ s when the injection stops; then, it decreases gradually due to particle deposition and those that are leaving through the exit register. Figure 2 also shows good agreement between the prediction of current hybrid RANS/LES model and those of the LBM-LES of [11] and LES of [31]. It is also observed that the present hybrid RANS/LES model predicts results as much close as to the LES results, thus somewhat improving the predictions of the LBM- $k-\epsilon$ model [11].

Figure 3 presents the predicted time variation of the number of suspended 10 μ m particles in the room as predicted by different models. It appears that the present hybrid model’s predictions are closer to the LBM-LES model’s results than those of the LBM- $k-\epsilon$ model are. When the trap boundary condition, which is more realistic for 10 μ m particles, is used, the number of suspended particles declines considerably, and the amount of reduction after 160 s reaches about 50%. In addition, the deviation between the predictions of the present hybrid LES/RANS model and the LES of Sajjadi et al. [11] is less than 4% for $t < 120$ s and is about 16% at $t = 145$ s.

For the trap boundary condition, the number of suspended 10 and 100 nm particles is shown in Figures 4 and 5. The trend of variations of the number of suspended particles shows the same pattern as those

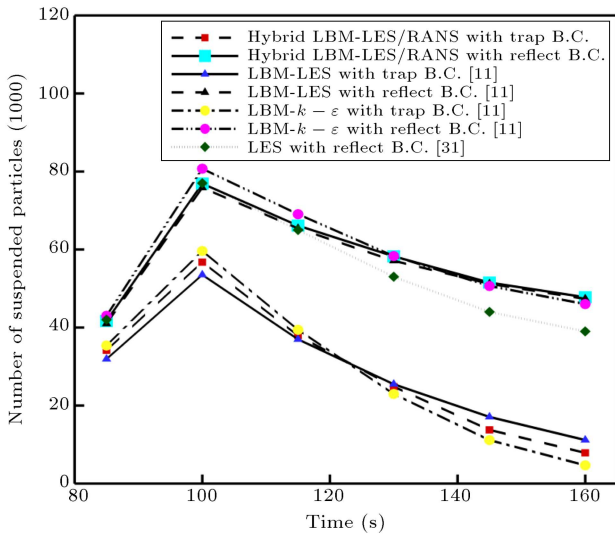


Figure 3. Comparison of the number of suspended 10 μm particles in the room under trap and reflect boundary conditions (total number of injected particles is 86,400 and Re_{Inlet} is 1628).

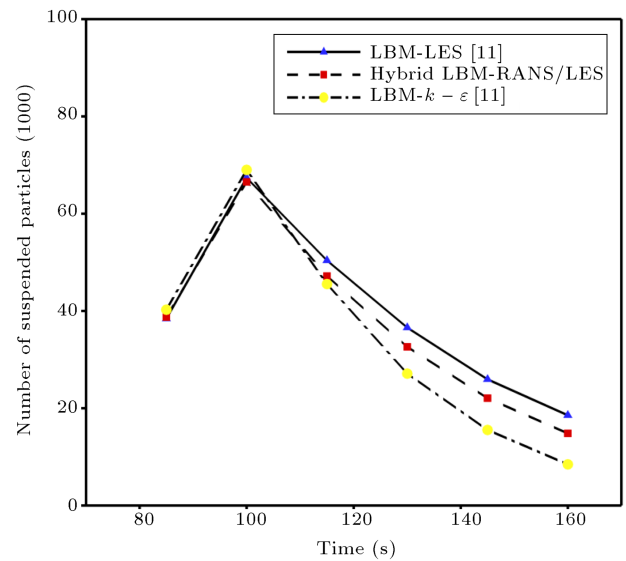


Figure 5. Comparison of the number of suspended 100 nm particles in the room under trap boundary condition (total number of injected particles is 86,400 and Re_{Inlet} is 1628).

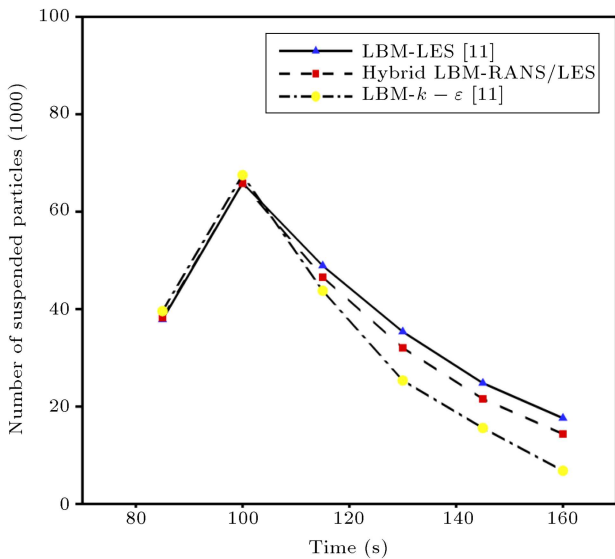


Figure 4. Comparison of the number of suspended 10 μm particles in the room under trap boundary condition (total number of injected particles is 86,400 and Re_{Inlet} is 1628).

of 1 and 10 μm particles. These figures also show that the hybrid model captures the dispersion and deposition of 10 and 100 nm particles more accurately than the $k - \epsilon$ model does. In addition, Figures 4 and 5 show that the $k - \epsilon$ model overestimates the particle deposition rate as discussed in [11,12] so that the number of suspended particles predicted by the $k - \epsilon$ model is less than the other models is. However, the hybrid model seems to achieve highly realistic results.

Figure 6 shows the time variation of the number of deposited particles on the different walls, as predicted by the hybrid model for 10 nm, 100 nm, 1 μm , and

10 μm particles. Figure 6(a) shows that the number of particles deposited on the ceiling increases with time roughly linearly. This is because, after injection, particles move up toward the outlet, and some particles reach the ceiling and depositing. This figure also shows that the smaller particles have a higher deposition rate on the ceiling than the larger ones do, due to the effect of gravity and higher Brownian motion.

Figure 6(b) shows that the number of deposited 10 μm particles on the floor is quite high, and more than 30% of the total injected 10 μm particles are deposited on the floor after 160 s. The amount of the deposition of 10 μm particles on the floor is of higher magnitude, as compared to particles of other sizes. This is due to the particle inertia in the inlet jet toward the floor and, also, the gravitational effect. The smaller particles with much lower inertia follow the airflow and are not deposited on the floor. In addition, Figure 6(b) shows that when the time reaches 100 s such that the particle injection stops, the slope of the deposition rate decreases. This is certainly the case for 1 μm particles and smaller ones. In addition, because of the Brownian excitation, the number of deposited 10 nm particles is slightly more than 100 nm and 1 μm particles.

Figure 6(c), (e), (f), and (g) show, respectively, the number of deposited particles on the right, front, back, and partition walls. It is seen that the cumulative deposition for these walls has the same trend; however, the rate of deposition varies with time and, also, for different particle sizes. After 120 s (20 s after the injection stops), the total deposition seems to saturate and does not change considerably.

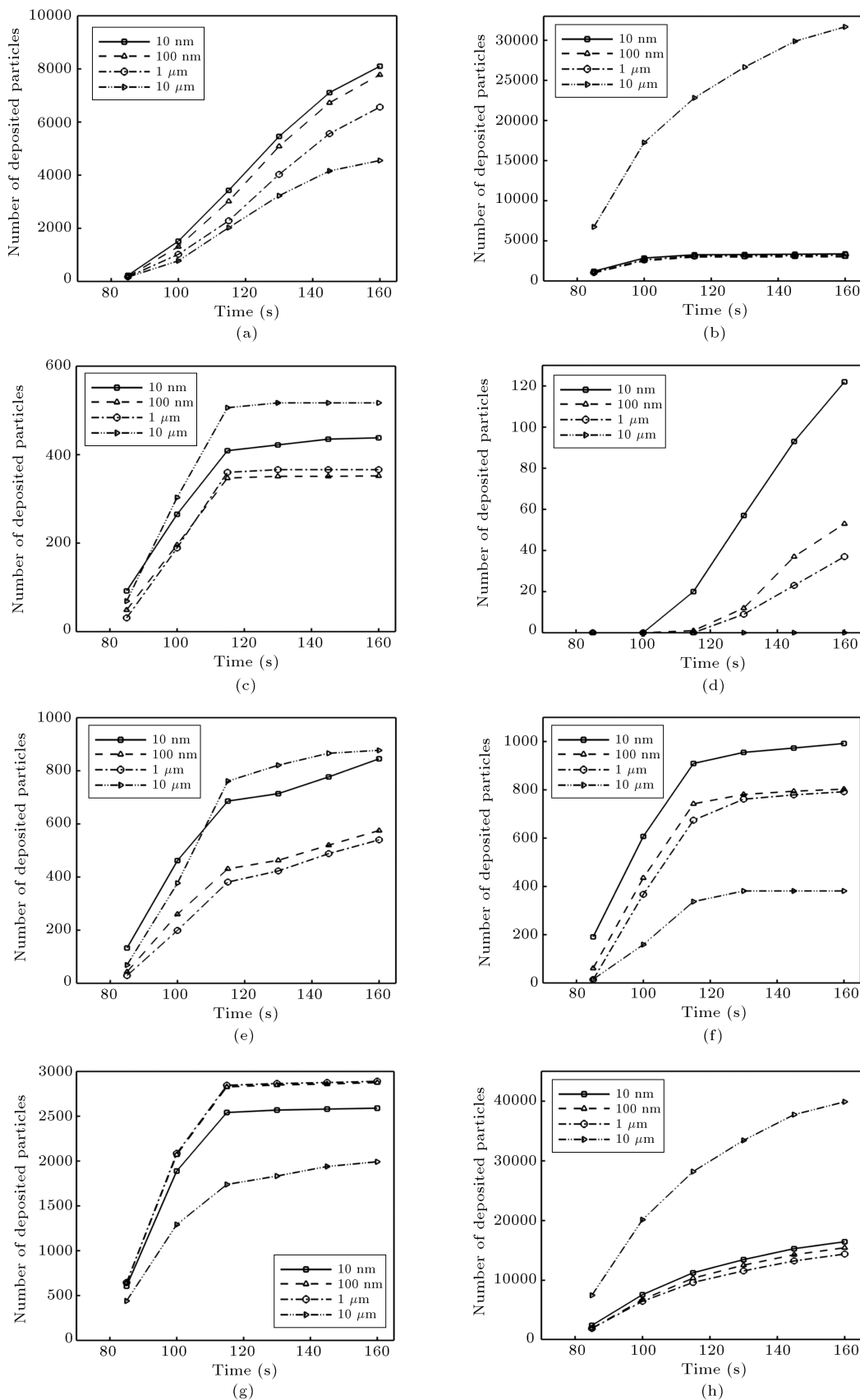


Figure 6. Number of deposited particles on the walls: (a) Ceiling, (b) floor, (c) right wall, (d) left wall, (e) front wall, (f) back wall, (g) partition, and (h) total for the hybrid RANS/LES model (total number of injected particles is 86,400 and Re_{Inlet} is 1628; trap boundary condition).

Figure 6(d) shows the total number of deposited particles of different sizes on the left wall. Up to $t = 100$ s (30 s after injection started), the deposition rate is zero for all sizes. After 100 s, a sufficient number of small particles are transported to the left side of the room, and the deposition on the left wall increases. This figure shows that the deposition for $10 \mu\text{m}$ particles on the left side is negligible. These trends are in contrast with deposition on the right wall, as shown in Figure 6(c). The reason is that a large fraction of $10 \mu\text{m}$ particles is deposited on the floor, the right wall, and the partition wall; a smaller fraction enters the left-hand side of the room.

The total number of deposited particles of different sizes on the walls are shown in Figure 6(h). As noted before, due to inertia and gravity, the deposition of $10 \mu\text{m}$ particle is more than other sizes. In addition, the deposition of 10 nm particles is more than 100 nm and $1 \mu\text{m}$ because of the higher intensity of the Brownian excitation.

Figures 7-10, respectively, show the total number of deposited particles on the walls of the room as predicted by different models for 10 nm , 100 nm , $1 \mu\text{m}$, and $10 \mu\text{m}$. It is seen that the deposition initiates after about 80 s and increases at different slopes for different sizes. The deposition rate of $10 \mu\text{m}$ is the highest due to the dominance of the impaction process. The Brownian motion causes somewhat higher deposition rates for 10 nm particles than that for 100 nm and $1 \mu\text{m}$ particles. For particles smaller than $1 \mu\text{m}$, Figure 7 shows that the LES model predicts the lowest deposition rates, while the $k - \varepsilon$ model predicts the highest. The predictions of the present hybrid model for the deposition are similar

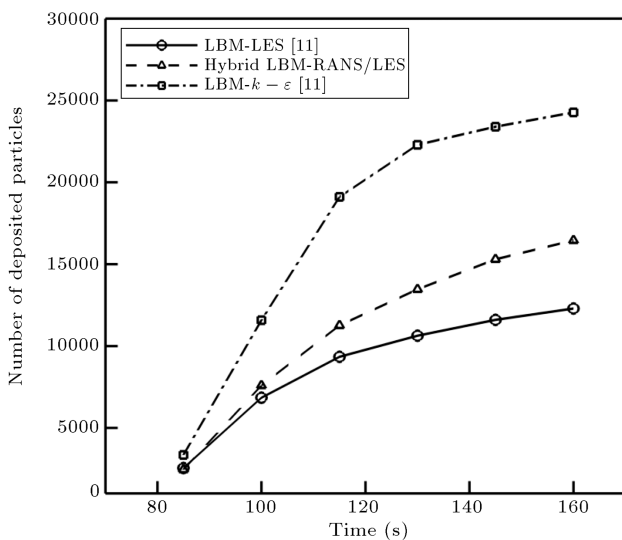


Figure 7. Comparison of the total number of deposited 10 nm particles on the walls of the room for various models (total number of injected particles is 86,400 and Re_{Inlet} is 1628; trap boundary condition).

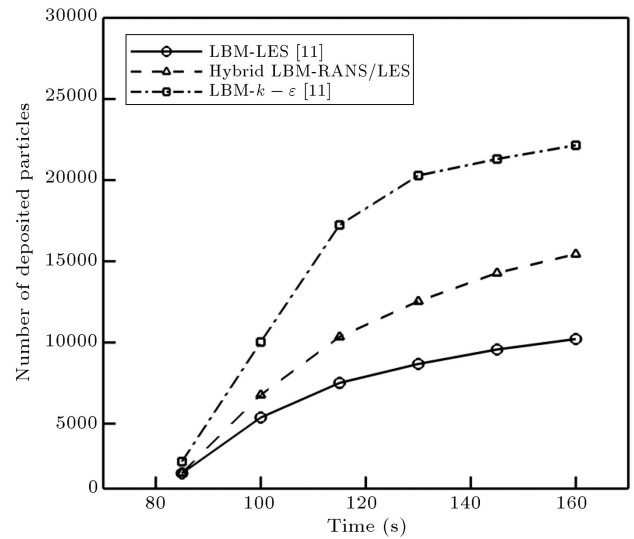


Figure 8. Comparison of the total number of deposited 100 nm particles on the walls of the room for various models (total number of injected particles is 86,400 and Re_{Inlet} is 1628; trap boundary condition).

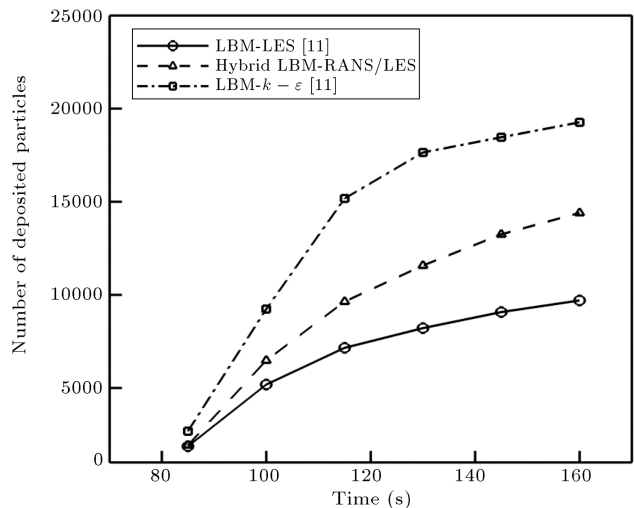


Figure 9. Comparison of the total number of deposited $1 \mu\text{m}$ particles on the walls of the room for various models (total number of injected particles is 86,400 and Re_{Inlet} is 1628; trap boundary condition).

between the two, yet are closer to the predictions of LES model. The over-prediction of the deposition rate by the $k - \varepsilon$ model is well known. Tian and Ahmadi [1] reported that the $k - \varepsilon$ model overestimated the deposition velocity in turbulent duct flows, since this model cannot properly capture the anisotropic turbulence fluctuations. They showed that accounting for the anisotropy of turbulence fluctuations and the near-wall effects can improve the results. Figures 7-9 show similar over-estimation patterns of the $k - \varepsilon$ model. However, by using the hybrid model, which can capture the fluctuation velocity in the bulk of the

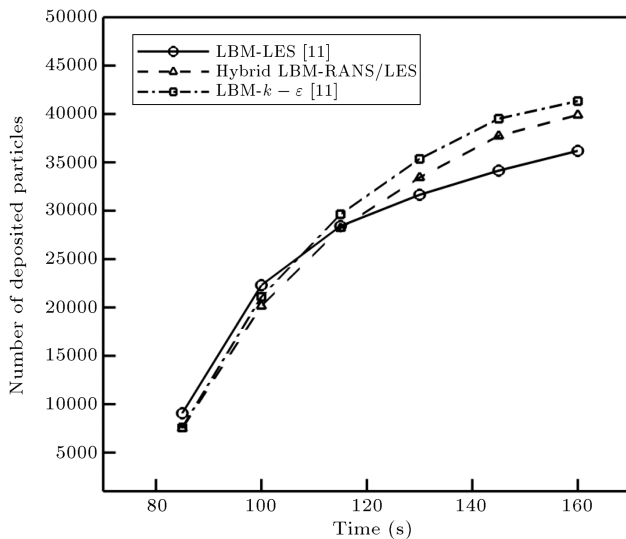


Figure 10. Comparison of the total number of deposited $10 \mu\text{m}$ particles on the walls of the room for various models (total number of injected particles is 86,400 and Re_{Inlet} is 1628; trap boundary condition).

domain correctly, the particle deposition decreases and is closer to the LES results.

For $10 \mu\text{m}$ particles, Figure 10 shows that the predictions of total deposition by the three models are closer to each other; however, similar but milder differences are seen. The reason is that for $10 \mu\text{m}$ particles, the impaction dominates the deposition process, and the influence of turbulence deposition becomes smaller.

6. Conclusions

The hybrid RANS/LES in conjunction with the lattice Boltzmann method was used to simulate particle dispersion and deposition in a room. For the LES model, the sub-grid scale turbulence effects were included in the Smagorinsky model. For using the $k - \epsilon$ turbulence model within the framework of LBM, the formulation was enhanced by the addition of two populations for k and ϵ . For the hybrid RANS/LES method, the near-wall region was simulated using the $k - \epsilon$ model, and the bulk of the flow region was analyzed by the LES model using the LBM. Deposition and dispersion of particles with diameters of 10 nm - $10 \mu\text{m}$ in a room were analyzed. Based on the presented results, the following conclusions are drawn:

- The predictions of the hybrid RANS/LES for particle deposition and dispersion are more accurate than that of RANS is, yet somewhat less accurate than the LES results. Average deviations of predictions of the present hybrid model and the RANS method for deposition of $10 \mu\text{m}$ particle in comparison with the LES results are, respectively, 8% and 12%.
- The $k - \epsilon$ model overestimates the deposition rate,

because this model cannot capture the anisotropy of turbulence fluctuations correctly.

- With the increase of particle diameter from 10 nm to $1 \mu\text{m}$, the total number of deposited particles in the room decreases by about 15% due to the decline of the intensity of the Brownian excitation.
- The number of depositions for $10 \mu\text{m}$ particle is more than other studied sizes. This is due to the gravitational sedimentation and inertial impaction.

Nomenclature

f_i	Density distribution functions
g_i	Turbulence kinematic energy distribution functions
h_i	Dissipation distribution functions
k	Turbulence kinematic energy
ϵ	Dissipation
ω_i	Weighted factor indirection i
τ_k	Relaxation time for k
τ_ϵ	Relaxation time for ϵ
λ	Molecular mean free path of the gas
d	Particle's diameter
g	Gravity acceleration
T	Fluid temperature
ρ	Density
ν	Kinematic viscosity

References

1. Tian, L. and Ahmadi, G. "Particle deposition in turbulent duct flows comparisons of different model predictions", *J. Aerosol Sci.*, **38**, pp. 377-397 (2007).
2. Wang, M., Lin, C.H., and Chen, Q. "Advanced turbulence models for predicting particle transport in enclosed environments", *Build. Environ.*, **47**, pp. 40-49 (2012).
3. Zhang, Z. and Chen, Q. "Comparison of the Eulerian and Lagrangian methods for predicting particle transport in enclosed spaces", *Atmospheric Environ.*, **41**(25), pp. 5236-5248 (2007).
4. Zhao, B., Zhang, Y., Li, X., Yang, X., and Huang, D. "Comparison of indoor aerosol particle concentration and deposition in different ventilated rooms by numerical method", *Build. Environ.*, **39**, pp. 1-8 (2004).
5. Sajjadi, H., Gorji, M., Hosseinzadeh, S.F., Kefayati, G.H.R., and Ganji, D.D. "Numerical analysis of turbulent natural convection in square cavity using large-eddy simulation in lattice Boltzmann method", *Ir. J. Sci. Tech. Tr. Mech. Eng.*, **35**, pp. 133-142 (2011).
6. Sajjadi, H., Gorji, M., Kefayati, G.H.R., and Ganji, D.D. "Lattice Boltzmann simulation of turbulent natural convection in tall enclosures using Cu/Water

- nanofluid”, *Numer. Heat Tr. A. Appl.*, **62**, pp. 512-530 (2012).
7. Holmes, S.A., Jouvray, A., and Tucker, P.G. “An assessment of a range of turbulence models when predicting room ventilation”, *Proce. of Heal. Build.*, **2**, Espo, Finland, pp. 401-406 (2000).
 8. Teixeira, C.M. “Incorporating turbulence models into the lattice-Boltzmann method”, *Int. J. Mod. Phys. C*, **9**, pp. 1159-1175 (1998).
 9. Succi, S., Chen, H., Teixeira, C., Bella, G., De Maio, A., and Molvig, K. “An integer lattice realization of a lax scheme for transport processes in multiple component fluid flows”, *J. Comput. Phys.*, **152**, pp. 493-516 (1999).
 10. Succi, S., Amati, G., and Benzi, R. “Challenges in lattice Boltzmann computing”, *J. Stat. Phys.*, **81**, pp. 5-16 (1995).
 11. Sajjadi, H., Salmanzadeh, M., Ahmadi, G., and Jafari, S. “LES and RANS model based on LBM for simulation of indoor airflow and particle dispersion and deposition”, *Build. Environ.*, **102**, pp. 1-12 (2016).
 12. Sajjadi, H., Salmanzadeh, M., Ahmadi, G., and Jafari, S. “Combination of lattice Boltzmann method and RANS approach for simulation of turbulent flows and particle transport and deposition”, *Particuology*, **30**, pp. 62-72 (2017).
 13. Chang, T., Hsieh, Y., and Kao, H. “Numerical investigation of airflow pattern and particulate matter transport in naturally ventilated multi-room buildings”, *Indoor Air*, **16**, pp. 136-152 (2006).
 14. Béghein, C., Jiang, Y., and Chen, Q. “Using large eddy simulation to study particle motions in a room”, *Indoor Air*, **15**, pp. 281-290 (2005).
 15. Zhang, Z. and Chen, Q. “Experimental measurements and numerical simulations of particle transport and distribution in ventilated rooms”, *Atmos. Environ.*, **40**, pp. 3396-3408 (2006).
 16. Jafari, S. and Rahnema, M. “Shear-improved Smagorinsky modeling of turbulent channel flow using generalized lattice Boltzmann equation”, *Int. J. Numer. Methods. Fluids*, **67**, pp. 700-712 (2011).
 17. Fernandino, M., Beronov, K., and Ytrehus, T. “Large eddy simulation of turbulent open duct flow using a lattice Boltzmann approach”, *Math. Comput. Simul.*, **79**, pp. 1520-1526 (2009).
 18. Sajjadi, H., Salmanzadeh, M., Ahmadi, G., and Jafari, S. “Turbulent indoor airflow simulation using hybrid LES/RANS model utilizing lattice Boltzmann method”, *Comput. Fluids*, **150**, pp. 66-73 (2017).
 19. Tessicini, F., Temmerman, L., and Leschziner, M.A. “Approximate near-wall treatments based on zonal and hybrid RANS-LES methods for LES at high Reynolds numbers”, *Int. J. Heat. Fluid. Fl.*, **27**, pp. 789-799 (2006).
 20. Jakirlic, S., Kadavelil, G., Kornhaas, M., Schäfer, M., Stenel, D.C., and Tropea, C. “Numerical and physical aspects in LES and hybrid LES/RANS of turbulent flow separation in a 3-D diffuser”, *Int. J. Heat. Fluid. Fl.*, **31**, pp. 820-832 (2010).
 21. Spalart, P.R., Jou, W.H., Stretlets, M., and Allmaras, S.R. “Comments on the feasibility of LES for wings and on the hybrid RANS/LES approach”, *Proc. of the First AFOSR Int. Conf. on DNS/LES*, Ruston, LA (1997).
 22. Temmerman, L., Hadzžiabdic, M., Leschziner, M.A., and Hanjali, K. “A hybrid two-layer URANS-LES approach for large eddy simulation at high Reynolds numbers”, *Int. J. Heat. Fluid. Fl.*, **26**, pp. 173-190 (2005).
 23. Papavergos, P.G. and Hedley, A.B. “Particle deposition behavior from turbulent flows”, *Chem. Eng. Res. Des.*, **62**, pp. 275-295 (1984).
 24. Li, A. and Ahmadi, G. “Dispersion and deposition of spherical particles from point sources in a turbulent channel flow”, *Aerosol Sci. Technol.*, **16**, pp. 209-226 (1992).
 25. Liu, D.L. and Nazaroff, W.W. “Particle penetration through building cracks”, *Aerosol Sci. Technol.*, **37**, pp. 565-573 (2003).
 26. Zhang, Z. and Chen, Q. “Prediction of particle deposition onto indoor surfaces by CFD with a modified Lagrangian method”, *Atmos. Environ.*, **43**, pp. 319-328 (2009).
 27. Fan, F. and Ahmadi, G. “A sub layer model for turbulent deposition of particles in vertical ducts with smooth and rough surfaces”, *J. Aerosol Sci.*, **24**, pp. 45-64 (1993).
 28. Zhang, H. and Ahmadi, G. “Aerosol particle transport and deposition in vertical and horizontal turbulent duct flows”, *J. of Fluid Mech.*, **406**, pp. 55-80 (2000).
 29. Salmanzadeh, M., Rahnema, M., and Ahmadi, G. “Effect of sub-grid scales on large eddy simulation of particle deposition in a turbulent channel flow”, *J. Aerosol Sci. Technol.*, **44**, pp. 796-806 (2010).
 30. Chen, Q. and Wang, M. “Modeling low velocity large scale fluctuating flows in ventilated space at transitional Reynolds numbers”, *ASHRAE Research Project (RP-1271)*, Purdue University (2009).
 31. Tian., Z.F., Tu, J.Y., Yeoh., G.H., and Yuen., R.K.K. “On the numerical study of contaminant particle concentration in indoor air flow”, *Build. Environ.*, **41**, pp. 1504-1514 (2006).

Biographies

Hasan Sajjadi received his PhD degree in Mechanical Engineering from the Shahid Bahonar University, Kerman, I.R., and is now an Assistance Professor of Mechanical Engineering at University of Bojnord, Iran. His research work concerns fluid mechanics, particle

deposition and dispersion, turbulent flow, and lattice Boltzmann method.

Mazyar Salmanzadeh received his PhD degree in Mechanical Engineering from the Shahid Bahonar University, Kerman, I.R, and is now an Associate Professor of Mechanical Engineering at Shahid Bahonar University, Iran. His research work concerns particle deposition and dispersion as well as turbulent flow.

Goodarz Ahmadi received his PhD degree in Mechanical Engineering from the Purdue University, West Lafayette, IN, USA and is now a Professor of Me-

chanical Engineering at Clarkson University, USA. His research work concerns particle transport, deposition and removal, aerosol mechanics, stochastic processes in engineering, advance theory of turbulence, and multiphase flow modeling.

Saeed Jafari received his PhD degree in Mechanical Engineering from the Shahid Bahonar University, Kerman, I.R, and is now an Associate Professor of Mechanical Engineering at Shahid Bahonar University, Iran. His research work concerns particle deposition and dispersion, turbulent flow, lattice Boltzmann method, and multiphase flow modeling.